

Broadband Terahertz Quantum Cascade Laser Dual-Comb Sources with Off-Resonant Microwave Injection

Xiaoyu Liao⁺ Ziping Li⁺ Wen Guan Kang Zhou Yiran Zhao Wenjian Wan Sijia Yang
Zhenzhen Zhang Chang Wang J. C. Cao* Heping Zeng* Hua Li*

⁺These authors contributed equally.

*Corresponding authors. Email: hua.li@mail.sim.ac.cn; jccao@mail.sim.ac.cn; hpzeng@phy.ecnu.edu.cn.

X. Liao, Dr. Z. Li, W. Guan, K. Zhou, Y. Zhao, Dr. W. Wan, S. Yang, Z. Zhang, C. Wang,
J. C. Cao, H. Li

Key Laboratory of Terahertz Solid State Technology, Shanghai Institute of Microsystem
and Information Technology, Chinese Academy of Sciences, Shanghai 200050, China

X. Liao, K. Zhou, Y. Zhao, S. Yang, C. Wang, J. Cao, H. Li

Center of Materials Science and Optoelectronics Engineering, University of Chinese Academy
of Sciences, Beijing 100049, China

W. Guan

School of Information Science and Technology, ShanghaiTech University, 393 Middle Huaxia
Road, Shanghai 201210, China.

H. Zeng

State Key Laboratory of Precision Spectroscopy, East China Normal University, Shanghai
200062, China.

Keywords: *terahertz quantum cascade laser, dual-comb, microwave injection*

Dual-comb spectroscopy has attracted increasing interests due to its unique advantages in high spectral resolution, fast detection, and so on. It is much demanding to develop broadband dual-comb sources covering absorption lines of various molecules for spectroscopic and imaging applications. Although the dual-comb technique is relatively mature in the infrared wavelengths, it is, currently, not commercially capable of practical applications in the terahertz regime due to the lack of high performance broadband terahertz dual-comb sources. In the terahertz frequency range, the electrically pumped quantum cascade laser (QCL), demonstrating high output power and good beam quality, is a suitable candidate for the dual-comb operation. However, free running terahertz QCL dual-comb sources normally show limited optical bandwidths ($\sim 100\text{-}200$ GHz). Although the resonant microwave injection locking has been widely used to broaden the emission spectra of terahertz QCLs by modulating the laser drive current at the cavity round-trip frequency, it is hard to be employed to broaden the dual-comb bandwidths due to the large phase noise induced by the resonant injection and non-ideal microwave circuits. Therefore, it is challenging to obtain broadband terahertz dual-comb sources that can fully exploits the laser gain bandwidth by utilizing the current resonant microwave injection. Here, we employ an off-resonant microwave injection to significantly broaden the dual-comb bandwidth of a terahertz QCL dual-comb source emitting around 4.2 THz. Under the off-resonant injection, the optical dual-comb bandwidth is significantly broadened from 147 GHz in free running to 620 GHz that is almost the double of the lasing bandwidth of the laser measured using a Fourier transform infrared spectrometer. The broadband dual-comb bandwidth is resulted from the injection locking and mutual locking effects induced by the off-resonant injection.

An optical frequency comb is a coherent radiation source consisting of a series of equally spaced frequency lines [1–5]. Due to its high stabilities in the frequency and time domains, the frequency comb has been widely used in various applications, e.g., spectroscopy, imaging, communications, and so on [6–9]. Among them, the dual-comb technique is a direct application of the frequency comb, and shows prominent advantages in the fast spectroscopy without a need of any moving part. In comparison, traditional infrared and terahertz spec-

trometers (for instance, the Fourier transform infrared and the time domain spectrometers) need mechanical scanning mirrors for obtaining a complete spectrum [10–12]. Extending the spectral coverage of frequency comb and dual-comb sources from infrared or visible wavelengths to other frequency ranges has been a key for fundamental research and industrial applications. The terahertz wave attracts progressive interests in last decades due to its unique characteristics, e.g., finger prints of vibrational and rotational absorptions of molecules, excellent transparency to many package materials, possible large bandwidth for communications, etc. However, the development of frequency comb and dual-comb sources in the terahertz frequency range is, currently, immature due to the lack of efficient terahertz radiation sources. The electrically pumped, semiconductor-based terahertz quantum cascade laser (QCL), with high output power, good far-field beam quality, and wide frequency coverage, is an ideal candidate for the frequency comb and dual-comb operation [13–16]. Regarding the terahertz QCL dual-comb operation, different architectures have been experimentally demonstrated, for instance, on-chip dual-comb, dual-comb spectroscopy using a fast detector, compact dual-comb spectrometer employing a self-detection scheme [17–22]. However, the measured dual-comb bandwidth, so far, is rather limited (less than 200 GHz). Similar to the technique of radio frequency (RF) injection at the laser round-trip frequency that has been used for a single laser to significantly broaden the emission spectrum, a microwave double injection has been also implemented onto a dual-comb platform. Because the strong resonant injection will introduce large phase noise and distort the dual-comb spectrum, no obvious broadening of dual-comb spectra has been observed. Therefore, it is still challenging to obtain a broadband terahertz dual-comb operation using the current RF technique.

Here, in this work we demonstrate an off-resonant microwave injection to significantly broaden the terahertz dual-comb bandwidth without bringing the sizable phase noise. The two terahertz QCL combs are fully separated. One of the lasers is used as a fast detector for the dual-comb detection. We reveal that the off-resonant microwave injection can significantly broaden the dual-comb bandwidth from 357 MHz (in free running without the RF injection) to 1.32 GHz (off-resonant injection at 19 dBm), corresponding to an optical bandwidth from 147 GHz to 620 GHz. The stability of the dual-comb source is evaluated by the phase noise measurement, the frequency and amplitude Allen deviations analysis. Finally, the spectroscopic ability of the terahertz dual-comb source is confirmed by a transmission measurement of a GaAs etalon sample.

Figure 1a shows the experimental setup of the off-resonant injection terahertz QCL dual-comb source (see Figure S1 in Supporting Information for a photograph of the experimental apparatus). The two QCLs are based on a hybrid active region design and processed into a single plasmon waveguide geometry (see Experimental Section). The dual-comb operation requires a slight difference between the two inter-mode beatnotes, f_{BN1} and f_{BN2} . However, f_{BN1} and f_{BN2} cannot differ too much. Otherwise, the generated dual-comb signal will be out of the detection bandwidth. In this work, to obtain an acceptable difference between f_{BN1} and f_{BN2} (tens of MHz), a nominally identical laser cavity length of 6 mm is implemented for both lasers. Due to the imperfections in cleaving and device fabrication processes, the two lasers, in principle, are not exactly identical, which finally results in a slight difference between f_{BN1} and f_{BN2} . The laser ridge width of 150 μm is selected because it is more favorable for the frequency comb operation when a given substrate thickness of 150 μm is used [23]. As shown in Figure 1a, the microwave injection is directly ap-

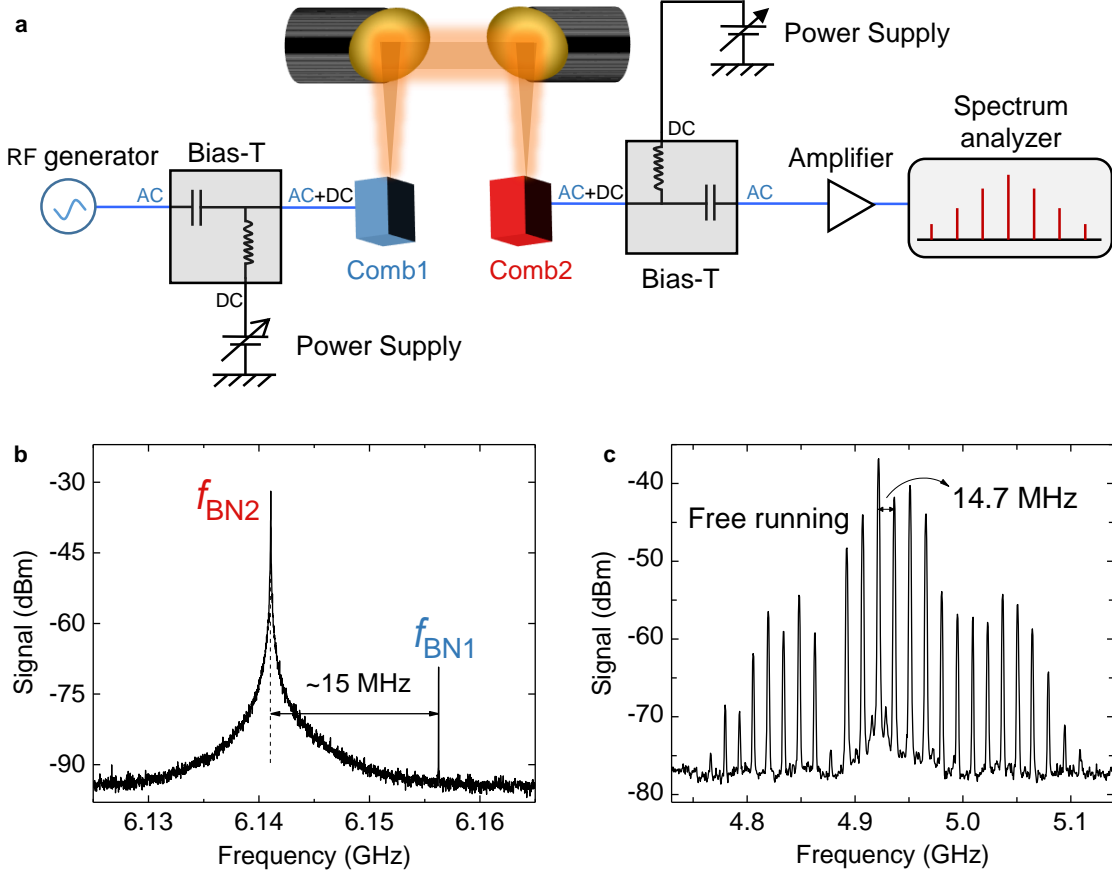


Figure 1: Experimental setup of the terahertz dual-comb source and dual-comb operation in free running. a) Experimental setup of the terahertz QCL dual-comb source with the microwave injection. Comb1 and Comb2 are terahertz QCLs with a ridge width of $150 \mu\text{m}$ and a cavity length of 6 mm. The RF generator injects microwave signals onto Comb1 via a Bias-T. The inter-mode beatnote and dual-comb signals are measured using Comb2 as a fast terahertz detector. b) Free running inter-mode beatnote signals measured using Comb2 as a detector with a resolution bandwidth (RBW) of 20 kHz and a video bandwidth (VBW) of 200 Hz. f_{BN1} and f_{BN2} are the inter-mode beatnotes of Comb1 and Comb2, respectively. The difference between f_{BN1} and f_{BN2} is around 15 MHz. c) Dual-comb spectrum measured when the two lasers are operated in free running. The measured line spacing is 14.7 MHz. The dual-comb spectrum was recorded with a RBW of 1 MHz and a VBW of 5 kHz. The results shown in (b) and (c) are recorded as Comb1 and Comb2 are operated at 990 mA at 30.1 K and 985 mA at 28.4 K, respectively.

plied onto Comb1. The injection conditions, i.e., resonant or off-resonant injections, and RF power, can be easily tuned by controlling the RF generator. In order to change the terahertz light coupling between Comb1 and Comb2, two parabolic mirrors are used. The beating of the two laser combs is self-detected using Comb2 as a detector. Note that the two laser combs have same functions, and therefore, the other laser (Comb1) can be also used as a detector for the dual-comb detection. Because the electron relaxation time in terahertz QCLs is fast in picoseconds, the QCL itself can be used as a fast detector for the multiheterodyne dual-comb detection with a bandwidth up to tens of gigahertz [24]. The RF signals including the inter-mode beatnote and dual-comb spectra are sent to the AC port of the Bias-T that is connected to Comb2, and then amplified using a microwave amplifier with a gain of 30 dB, and finally registered on a spectrum analyzer.

To prove the dual-comb operation, we show the inter-mode beatnotes of Comb1 and Comb2 (f_{BN1} and f_{BN2}), and the dual-comb spectrum obtained without any microwave perturbations in Figures 1b and 1c, respectively. In free running, when the two lasers are electrically pumped at currents of 990 mA (Comb1) and 985 mA (Comb2), two narrow inter-mode beatnote lines (f_{BN1} and f_{BN2}) can be obtained with a frequency difference of ~ 15 MHz. This frequency difference determines the line spacing of the dual-comb spectra. Indeed, as shown in Figure 1c, the measured dual-comb spectrum centered around 4.95 GHz demonstrates a line spacing of 14.7 MHz which is in agreement with the measured frequency difference as shown in Figure 1b. Note that the 300 kHz mismatch is due to the frequency drift during the measurement. The dual-comb spectrum in Figure 1c spans over 357 MHz with 25 lines, which corresponds to an optical bandwidth of ~ 140 GHz by considering the repetition frequency of the laser combs. The dual-comb setup shown in Figure 1a is flexible for the optical coupling tuning compared to the experimental setup used in ref. [20] where two lasers are mounted on a same sample holder and the optical coupling between the two lasers cannot change once they are mounted. As shown in Figure S2 in Supporting Information, by changing the position of Comb2 along the optical axis, we are able to tune the optical coupling between the two laser combs. It can be clearly seen that the inter-mode beatnotes (f_{BN1} and f_{BN2}), dual-comb line number, dual-comb line spacing can be systematically tuned by changing the optical coupling.

Figure 2 demonstrates the effect of microwave injection on the terahertz dual-comb laser source. The experimental results obtained as the lasers are operated in free running (RF off) are also shown for a clear comparison. In Figure 2a, we show the dual-comb evolution as the injection condition is changed. The resonant microwave injection at 6.15499 GHz with 0 dBm RF power is first applied, which shows limited effects on the dual-comb bandwidth compared with that obtained in free running. As the RF power is increased to 5 dBm, actually the dual-comb signal disappears immediately or signals with a broad pedestal are observed. It indicates that high power RF injection brings about large phase noise, which damages the coherence of the terahertz modes. Similar phenomena were also found in an on-chip dual-comb source under a microwave injection [22]. In order to bring back the dual-comb signal, we introduce the off-resonant microwave injection (i.e., the injection frequency is far away from the repetition frequencies of the comb lasers) as the RF power is greater than 5 dBm. It can be clearly seen from Figure 2a that by implementing the off-resonant microwave injection, we obtain not only stable dual-comb operation but also broad dual-comb bandwidths. Especially, when we inject at 6.34299 GHz (~ 200 MHz away from f_{BN2}) with a 19 dBm power, the optical bandwidth can reach 620 GHz with more than 90 lines, which is more than 3 times larger than the optical bandwidth measured in free running (147 GHz). To prove that the measured broad dual-comb bandwidth (620 GHz) is resulted from the optical coupling of the two laser combs rather than some fake signals from electronic crosstalks, in Video 1 (Supporting Information) we show the real-time dual-comb operation when a metal board is used to block the terahertz beams. It can be clearly seen that when the optical coupling is blocked, the dual-comb signal disappears immediately.

Different from the resonant injection where the inter-mode beatnote frequency (or repetition frequency) is firmly locked at the injecting microwave frequency and the locking range is in a level of dozens of megahertz depending on the power of the injecting microwave signal (see Figure S3 in Supporting Information), the off-resonant injection cannot firmly lock

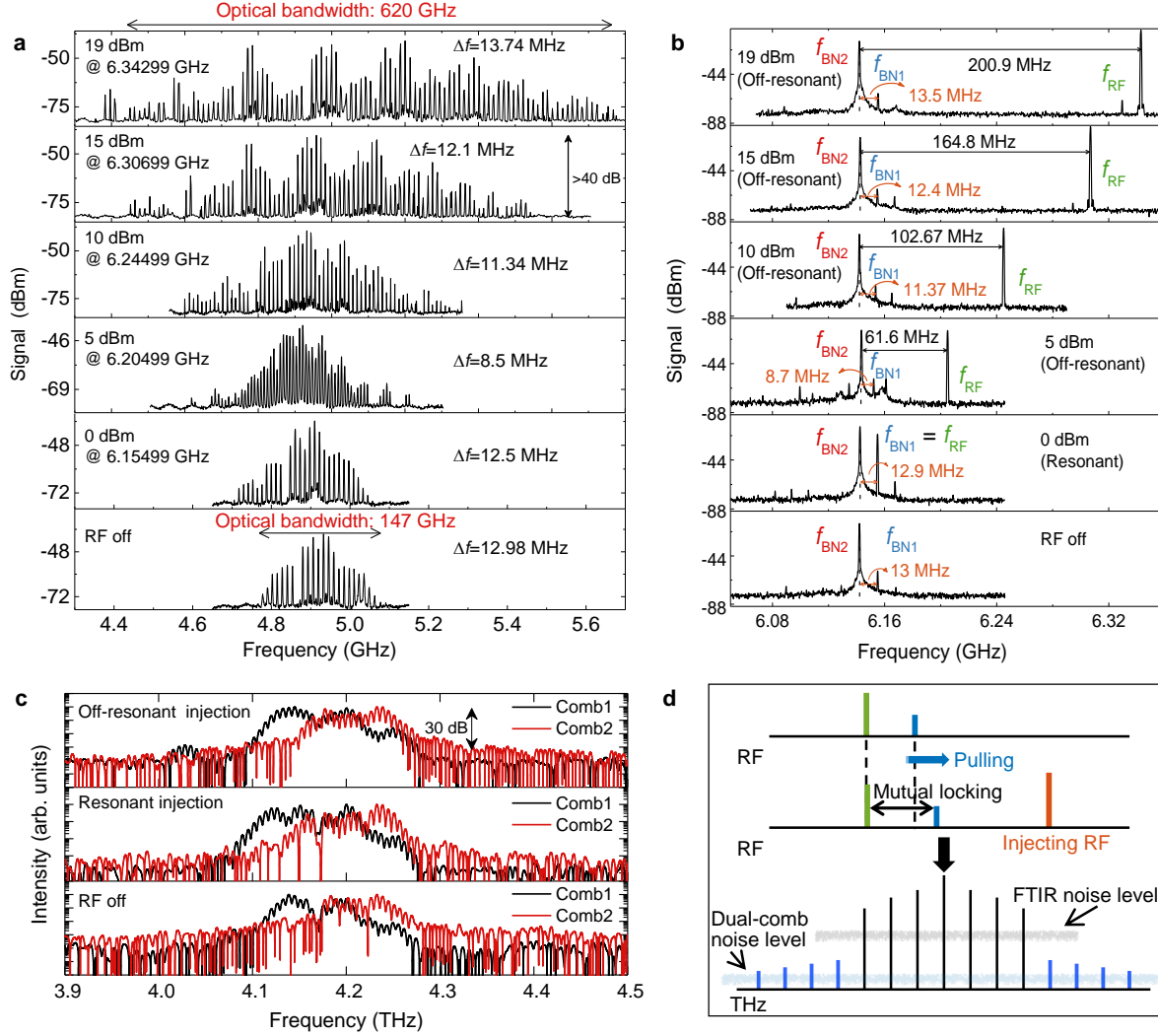


Figure 2: Broadband dual-comb operation with off-resonant microwave injection. a) Dual-comb spectra measured with various microwave injection conditions. As a reference, the dual-comb spectrum in free running (RF off) is shown in the lowest panel. From bottom to top, the injection condition changes from low power resonant injection to high power off-resonant injection. All data were recorded with a RBW of 1 MHz and a VBW of 5 kHz. Δf represents the measured dual-comb line spacings. b) Corresponding inter-mode beatnote and injecting RF signals (f_{RF}) measured with a RBW of 300 kHz and a VBW of 20 kHz. c) Emission spectra of the two terahertz QCLs measured in different injection conditions. Resonant injection: 0 dBm @ 6.15615 GHz for Comb1; 0 dBm @ 6.14212 GHz for Comb2. Off-resonant injection: 19 dBm @ 6.34299 GHz for both laser combs. The spectral resolution of 0.08 cm^{-1} is used for the emission measurement. d) Upper panel: Schematic demonstration of the two injection mechanisms, i.e., injection locking (pulling) and mutual locking, induced by the off-resonant injection. The blue and green lines represent f_{BN1} and f_{BN2} , respectively, and the red line is the injecting microwave signal (f_{RF}). Lower panel: Schematic plot of the comparison of noise levels of the FTIR and dual-comb measurements.

the laser beatnote to the injecting frequency because the two frequencies are far away from each other. As shown in Figure 2b, under the off-resonant injection condition, f_{BN1} and f_{BN2} are still around 6.15 GHz and the difference between them determines the dual-comb line spacing (see Figure 2a). Although the off-resonant injection cannot firmly lock the beatnote frequency, it still affects the beatnotes f_{BN1} and f_{BN2} . In Figure S4 (Support-

ing Information), the evolution of f_{BN1} and f_{BN2} with the change of injection condition is plotted. Under the off-resonant injection, with the increase of the RF power, an obvious pulling effect can be clearly observed, which is a sign that the locking mechanism starts to work. From Figure 2b, we can also observe that the sidebands beside the two beatnotes becomes stronger as the RF injection is applied, which indicates an increased interaction (mutual locking) between the two beatnotes. Therefore, the off-resonant injection can, in principle, partially lock the two inter-mode beatnotes, f_{BN1} and f_{BN2} . The data shown in Figures 2a and 2b were recorded using Comb2 as a detector. As we already explained previously, in principle, the other laser can be also used as a detector for the dual-comb detection. In Figure S5 (Supporting Information), we show the dual-comb and corresponding beatnote spectra measured using Comb1 as a detector under different injection conditions. We further show that as the power of the resonant injection is increased to a level (14 dBm), the coherence of the comb operation will be damaged and then the dual-comb spectrum disappears immediately (see Video 2 in Supporting Information). Because each laser has slightly different detection capability and the optical coupling strength can be different when using different lasers as detectors, we see the dual-comb results shown in Figure 2a and Figure S5a in Supporting Information are not identical.

The broadening of the dual-comb bandwidth shown in Figure 2a is resulted from the broadening of the terahertz emission spectra of the two laser combs under the off-resonant microwave injection. In Figure 2c, we show the terahertz emission spectra of the laser combs under different conditions, i.e., RF off (lower panel), resonant injection with 0 dBm power (middle panel), and off-resonant injection with 19 dBm power (upper panel), measured using a Fourier transform infrared (FTIR) spectrometer (see Experimental Section). Compared to the emission spectra measured in free running (RF off), a slight spectral broadening can be observed once the microwave injection (either resonant or off-resonant) is applied. The lasing region is measured between 4.1 and 4.3 THz with a lasing bandwidth of 200 GHz. The results shown in Figure 2c indicate that the microwave injection can broaden the emission spectra of the QCL combs. However, the lasing bandwidth measured from the FTIR is far less than the optical bandwidth of 620 GHz measured from the dual-comb spectrum shown in Figure 2a. The bandwidth discrepancy between the FTIR and the dual-comb measurements can be explained as follows. First of all, in the two measurements the detectors show different performances. In the FTIR setup, a far-infrared deuterated triglycine sulfate (DTGS) detector was used for the detection of the terahertz signal and the noise equivalent power (NEP) of the detector is in a level of $\text{nW}/\text{Hz}^{1/2}$. While, the QCL detector demonstrates a NEP in tens of $\text{pW}/\text{Hz}^{1/2}$ [22], which shows much stronger abilities for detecting weak signals than the DTGS detector. Therefore, some generated terahertz modes resulted from the off-resonant injection that are below the noise level of the FTIR can be still detectable by using the dual-comb setup. On the other hand, it is worth noting that the QCL configurations in the two measurements are different. In the dual-comb measurement, the two terahertz QCLs are optically coupled (see Figure 1a); while in the FTIR measurement, each time only one QCL is switched on and its light is directly sent to the FTIR chamber for spectral measurements. Although pump conditions, i.e., drive current and RF injection, are identical for the dual-comb and FTIR measurements, the optical feedback situations in the two measurements are entirely different. We are inclined to believe that the optical feedback in the dual-comb measurement geometry contributes to the broadening of the optical bandwidth. Because of the above-mentioned two reasons, we ob-

serve much wider optical bandwidth measured from the dual-comb measurement than that obtained from the FTIR measurement.

Here, we give more elaborations on the broadening mechanisms of the dual-comb bandwidth under the off-resonant microwave injection. As shown in Figure 2d, two locking mechanisms resulted from the off-resonant injection can, in principle, contribute to the significant bandwidth broadening. The first one is the direct injection locking of f_{BN1} , which is known as a powerful tool to significantly broaden the emission spectra of QCLs [24–26]. This injection locking mechanism can be proved by the pulling effect observed by increasing the injecting RF power (see Figure 2b and Figure S3 in Supporting Information). As the power of the injecting RF is increased, we can see f_{BN1} is pulled by the injecting RF signal, which is the phenomenal sign of the start of injection locking [22, 27]. The other mechanism is the mutual locking effect, which can be often observed in the optical injection locking experiment where two optical frequencies with a slight frequency difference inject with each other and finally the two frequencies will be locked together. Here as shown in Figure 2b, even in free running mode (RF off), we can see the generated weak sidebands on the right of f_{BN1} and on the left of f_{BN2} , which is resulted from the optical interactions of the two terahertz beams. Furthermore, as the external RF signal is applied and the RF power is increased gradually, we can see the generated sideband on the right side of f_{BN1} becomes stronger. It indicates that the mutual locking mechanism takes effect as the RF injection is applied. Different from the traditional optical injection locking, the mutual locking doesn't lock the two repetition rates (f_{BN1} and f_{BN2}) together and we can still observe two separate repetition frequencies as shown in Figure 2b. The two locking mechanisms, i.e., injection locking and mutual locking, function simultaneously and finally result in the broadening of the emission spectra as shown by the blue lines in Figure 2d. Due to the optical bandwidth discrepancies between FTIR and dual-comb measurements (see Figures 2a and 2c), we assume that the mutual locking that is absent in the FTIR measurement plays a vital role in the bandwidth broadening. It is worth noting that for either the injection locking or mutual locking, the deep-level mechanism for the broadening is the four-wave mixing locking. The four-wave mixing is the inherent and important mechanism to generate equidistant frequency lines in the nonlinear GaAs gain medium. We assume that both injection locking and mutual locking can largely enhance the four-wave mixing locking effect in the QCLs, which then significantly broaden the emission spectra of the QCL combs. Finally, we observe the dual-comb line proliferation and bandwidth broadening as shown in Figure 2a. In this work, the measured maximum dual-comb bandwidth is equivalent to an optical bandwidth of 620 GHz that is close the double of the lasing bandwidth (330 GHz) measured from a 6-mm-long laser with an identical active region structure [28]. If we assume the gain bandwidth is a double of the lasing bandwidth as experimentally testified for a QCL emitting around 2.5 THz [29, 30], the obtained 620 GHz optical bandwidth in this work almost reaches limit of the gain bandwidth of the laser active region.

To further prove the dual-comb line proliferation induced by the off-resonant injection is resulted from the mode proliferation in the terahertz range, transmission measurements of a known absorber (filter) are carried out employing the dual-comb setup. The blue curve in Figure 3a is the measured transmission (using FTIR) of the filter used in this study by taking ratios of the data of the red curve to those of the black curve. It can be seen that the filter is not narrow-band and its bandpass region is not precisely located in the optical range of the QCL combs. However, the high frequency tail of the filter fully covers the

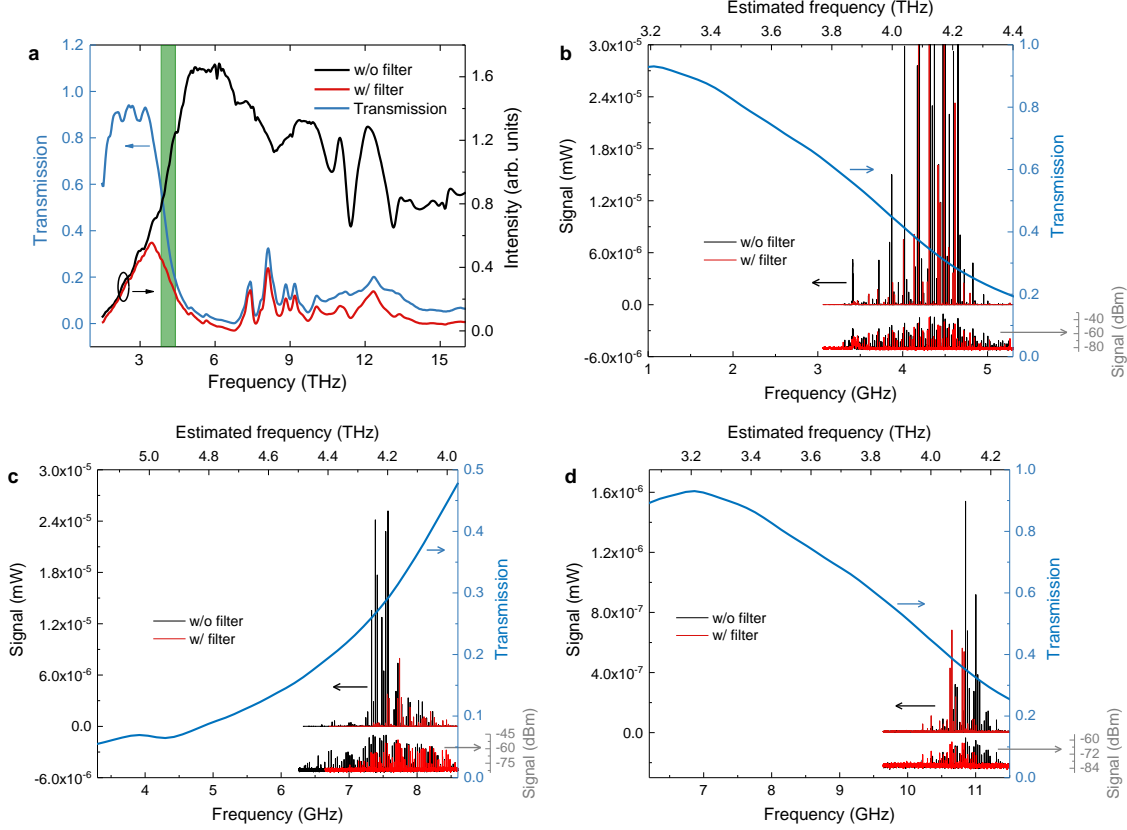


Figure 3: Dual-comb measurements of a filter. a) Transmission spectrum (blue curve) of the selected band-pass filter obtained by taking ratios of the data of the red curve to those of the black curve. All data were recorded using a FTIR spectrometer. The green shaded area approximately indicates the operation frequency range of the QCL combs (3.8-4.4 THz). b), c), d) are dual-comb spectra measured without (black curves) and with (red curves) the filter at different carrier frequencies in the microwave regime. Their carrier frequencies are around 4, 8, and 11 GHz in b), c), and d), respectively. The left y-axes show the dual-comb signal in a unit of mW, while the grey right y-axes show the dual-comb power in a unit of dBm. The top x-axes show the estimated frequencies in THz which correspond to the frequencies in microwave (bottom x-axes). The blue curves which are bounded to the blue right y-axes and top x-axes show the measured transmission spectra of the filter for comparison. For measurements shown in b)-d), the data were recorded with a RBW of 100 kHz as Comb1 is operated at 1070 mA at 26 K and Comb2 is operated at 1150 mA at 30 K. Comb1 is under the off-resonant injection situation (see the top panel of Figure 2a).

operation frequency range of the QCLs from 3.8 to 4.4 THz (see the shaded area in Figure 3a). The slope showing the decrease in transmission with increasing frequency can be employed to identify if the generated comb lines are real or fake. The main idea is that when the filter is placed in the beam path of the dual-comb setup, the dual-comb spectra will be affected due to the frequency-dependent absorption (or transmission) of the filter. By comparing the dual-comb spectra without and with the filter, we, in principle, can prove if the dual-comb lines are generated from the beats of the modes in the terahertz range.

To perform the measurement, Comb1 is under the off-resonant injection situation. We first record the dual-comb spectra using Comb2 as a detector with the beam path purged with nitrogen and then record the dual-comb spectra with the filter placed in the beam path of the dual-comb setup for comparison. The main results are shown in Figures 3b, 3c, and 3d

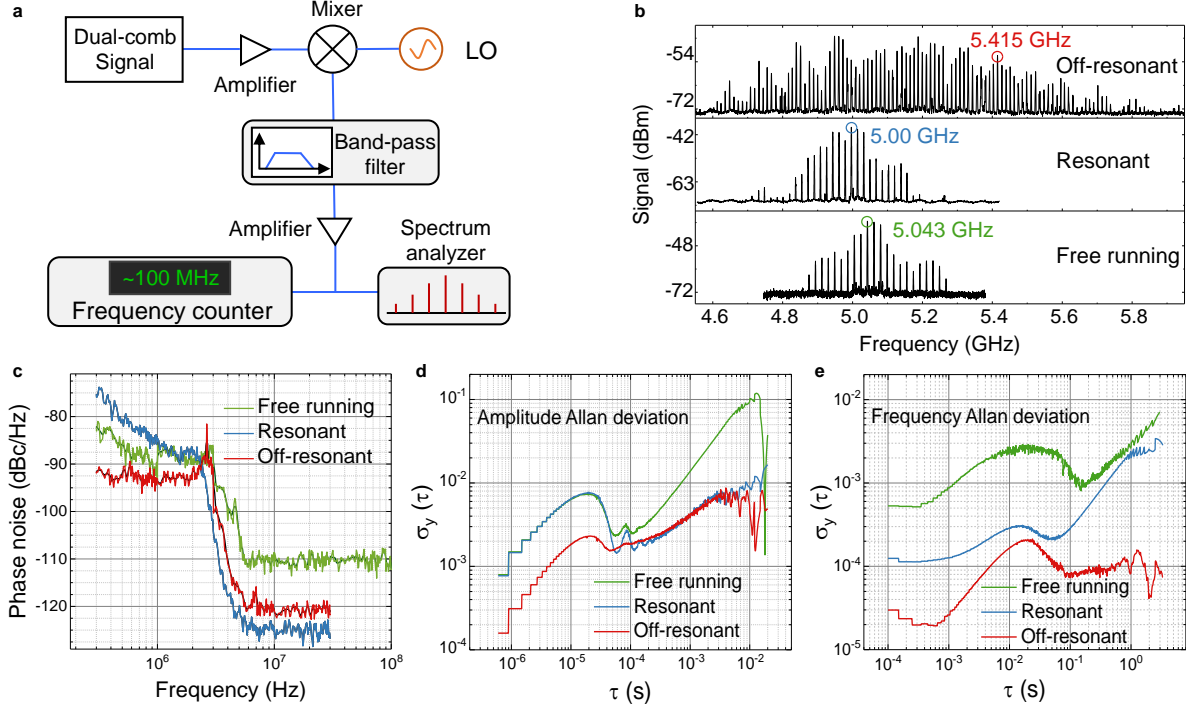


Figure 4: Stability evaluation of the dual-comb signals at different conditions. a) Experimental setup of the Frequency Allan deviation analysis for the dual-comb signals. To record the frequency as a function of time, the dual-comb signals should be converted to low frequencies within the bandwidth of the frequency counter. LO: Local oscillator signal (100 MHz difference from the selected signal). b) Dual-comb spectra measured with a RBW of 1 MHz in free running, resonant injection, and off-resonant injection. The circles mark the dual-comb lines that are selected for the stability evaluation. (c), (d) and (e) are measured phase noise spectra (RBW: 10%, tolerance: 10%), frequency Allen deviation, and amplitude Allen deviation of the lines marked in b, respectively. All the data were recorded when Comb1 and Comb2 are operated at 990 and 985 mA, respectively.

for the dual-comb spectra recorded at carrier frequencies around 4, 8, and 11 GHz, respectively. Because different beats of the two QCL comb lines can generate dual-comb signals at different carrier frequencies, in Figures 3b-3d, we show three sets of dual-comb spectra at three lowest microwave carrier frequencies. As we already illustrated in ref. [20], the microwave-terahertz frequency link for two neighbouring sets of dual-comb lines shows opposite trend, i.e., if for one set of dual-comb lines, the increase in microwave frequency corresponds to an increase in terahertz, then for the neighbouring sets of dual-comb lines, the increase in microwave frequency will correspond to a decrease in terahertz. Because of this, one can find that the microwave-terahertz link shown in Figure 3c shows opposite trend as those shown in Figures 3b and 3d. To help analyze the data, we plot the transmission of the filter as a reference in Figures 3b-3d. It can be clearly seen that for all cases, the dual-comb results show good agreements with the measured transmission of the filter. In the higher terahertz frequency tail, the dual-comb lines are strongly attenuated or even removed due to the stronger absorption (or smaller transmission) in the higher terahertz frequency range. Therefore, the dual-comb measurements of the filter can qualitatively prove that the significant broadening of the dual-comb bandwidth is resulted from the proliferation of the terahertz modes due to the off-resonant microwave injection.

The stability of the dual-comb signals is important for practical applications. In Figure 4, we evaluate the stability of the dual-comb signals obtained in different situations, i.e., free running mode, resonant injection and off-resonant injection. Figure 4a plots the experimental setup for the frequency stability measurement. To meet the bandwidth requirement of the frequency counter, the dual-comb signal is down-converted from 5 GHz to 100 MHz and then only one dual-comb line is finally selected using a band-pass filter for the frequency stability measurement (see Experimental Section for details). In Figure 4b, from bottom to top panels we show three dual-comb spectra recorded in free running, resonant injection and off-resonant injection situations. As indicated by the circles, three typical lines located at 5.043 GHz (free running), 5.00 GHz (resonant injection), and 5.415 GHz (off-resonant injection) are chosen for the stability evaluation. Figures 4c, 4d, and 4e plot the phase noise spectra, amplitude Allan deviation, and frequency Allan deviation, respectively, for the three lines indicated by the circles in Figure 4b. As expected, the phase noise and Allan deviation plots obtained in the injection condition show improved values than those measured in free running mode.

Note that an effective way to further improve the stability of the dual-comb system is to phase lock the frequency lines. The locking of a single QCL comb has been already demonstrated by locking its repetition rate using either microwave injection or a saturable absorber, as well as by locking the carrier offset frequency using a highly stable femtosecond laser [6, 31–33]. However, the complete locking of a dual-comb source needs all four frequencies (two repetition rates and two carrier offset frequencies) to be locked simultaneously, which will significantly complicate the system. In ref. [34], we demonstrated the locking of terahertz QCL dual-comb source by phase locking one of the dual-comb lines to a stable microwave oscillator without any control of the repetition rate and carrier offset frequency of individual laser comb. Although just one dual-comb line is phase locked, we find that the stability of other dual-comb lines is significantly improved. In this work, we also applied the locking technique onto the dual-comb source investigated here. In Figure S6a (Supporting Information), we show the experimental setup of the phase locking. We first down-convert the dual-comb signal to low frequencies and then one of the dual-comb lines is selected for the phase locking. The Servo signal is used to dynamically control the drive current of one of the comb lasers to finally keep the dual-comb lines stable. The experiment shows that we can easily lock the repetition rate of one of the lasers (see Figure S6b and Video 3 in Supporting Information). However, the long-term locking of the dual-comb signal cannot be obtained. From Video 4 in Supporting Information, we can see that the phase locking of the dual-comb source can work for a short period (around 9 seconds) then we lost it. In ref. [34], the two laser combs sit on a same sample holder in a cryostat, while in this work the two laser combs are completely separated and they don't share the same temperature fluctuations. Therefore, it is more difficult to obtain a stable phase-locking of the dual-comb source in this work. As can be seen from Video 4 in Supporting Information, the frequency drift of the dual-comb lines is almost on the borderline of the locking bandwidth of the phase locked loop (PLL). It, in principle, should be feasible to achieve the phase locking by further optimizing the Servo electronics to slightly increase the locking bandwidth of the PLL.

To further verify the spectroscopic ability of the dual-comb source, we carried out the transmission measurement of a GaAs etalon employing the dual-comb source under off-resonant injection. To perform the transmission measurement, we just simply insert the sample in

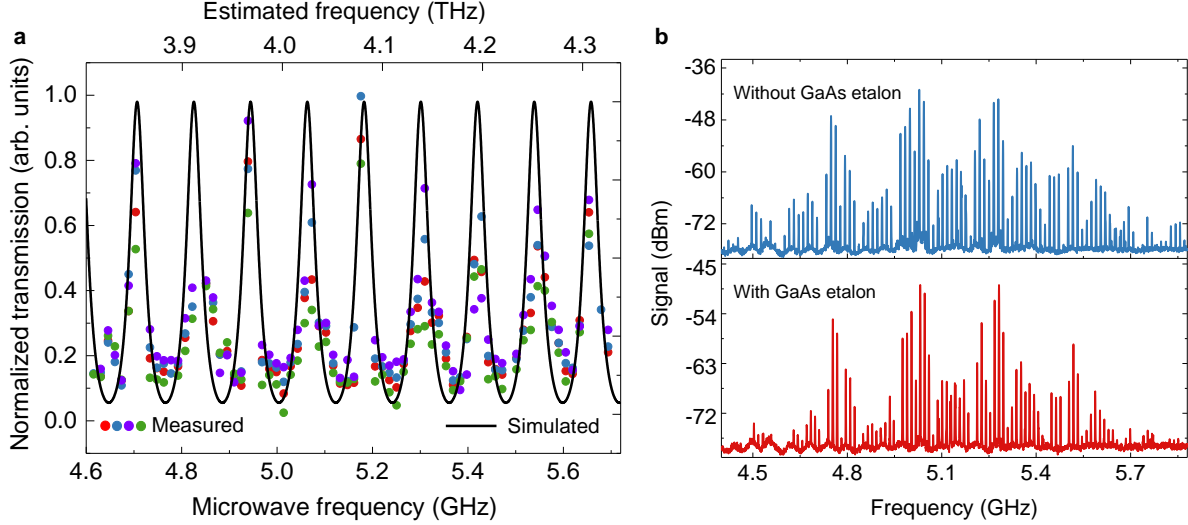


Figure 5: Transmission of a GaAs etalon sample measured using the terahertz dual-comb source with off-resonant injection. a) Transmission spectrum of a GaAs etalon sample ($625 \mu\text{m} \pm 25 \mu\text{m}$). The circles (bottom axis) with different colors are experimental results measured at different times while the black curve (top axis) is a fit. b) Dual-comb spectra with and without the GaAs etalon sample. The off-resonant injection at 6.34299 GHz with a power of 19 dBm is applied onto Comb1.

the parallel beam between the two parabolic mirrors (see Figure 1a) and then record the dual-comb spectrum in real-time. Figure 5a plots the normalized transmission of a $625 (\pm 25) \mu\text{m}$ thick GaAs etalon. The red dots are experimental results that are obtained by taking ratios of the peak intensities of the dual-comb spectra measured with and without the GaAs etalon sample (see Figure 5b). The black curve is the transmission fit calculated by considering a refractive index of 4.065 and a sample thickness of $678 \mu\text{m}$. It is known that the inter-mode beatnote frequency f_{BN} of a laser follows the following relation, i.e., $f_{\text{BN}} = c/2ln$ where c is the speed of light in vacuum, l is the laser cavity length, and n is the refractive index. In this work, l is equal to 6 mm and we roughly set f_{BN} as the average value of $f_{\text{BN}1}$ and $f_{\text{BN}2}$ as shown in Figure 1b. Finally the refractive index parameter of 4.065 is obtained and then used for the fitting. Note that the sample thickness used for the fitting is slightly thicker than the nominal value, which can be attributed to the sample tilt during the measurement. Although the dual-comb spectrometer shows an optical bandwidth of 620 GHz for air, its practical optical bandwidth is around 480 GHz when a GaAs sample is loaded as shown in Figure 5a. As a proof of concept, the results shown in Figure 5a indicate that the broadband terahertz dual-comb source under off-resonant injection is capable of spectroscopic applications.

In summary, we have demonstrated a broadband terahertz quantum cascade laser dual-comb operation with off-resonant microwave injection. By exploiting the injection locking and mutual locking mechanisms which largely enhances the four-wave mixing locking effect in the QCL combs), the optical bandwidth of the dual-comb source can reach 620 GHz under an off-resonant microwave injection with a power of 19 dBm, which is three times larger the optical bandwidth obtained in free running mode. The phase noise and Allan deviation analysis showed that the microwave injection can improve the stability of the dual-comb source. Finally, the transmission of a GaAs etalon sample was measured, which further confirmed the spectroscopic ability of the terahertz dual-comb source under the off-

resonant microwave injection.

Experimental Section

Terahertz QCLs and emission spectral measurement: The terahertz QCL used in this work is based on a hybrid active region structure that combines the bound-to-continuum optical transitions and the resonant phonon scattering for depopulation of the lower laser state. The details of the layer structure can be found in ref. [28]. The entire QCL active region is grown using a molecular beam epitaxy system on a semi-insulating GaAs (100) substrate. The grown wafer is then processed into single plasmon waveguide laser ridges. The ridges are cleaved into laser bars with cavity lengths ranging from 2 to 6 mm and then indium-soldered onto copper bases (heat sink). Finally, the QCL device is mounted onto a cold finger of a cryostat for electrical and optical measurements.

It is worth mentioning that in this work the deployment of the single plasmon waveguide can benefit the optical coupling between the two laser combs. It is known that the optical mode can go further into the substrate in the single plasmon waveguide QCL, while for the double-metal waveguide the mode is confined in the active region between two metal layers. Therefore, when the terahertz light emitted from one QCL is coupled into the other QCL (detection comb) via the device facet, the single plasmon waveguide can couple more light into the detector for the multiheterodyne dual-comb detection because it has much larger effective facet area for the optical interaction than the double-metal waveguide [20]. The emission measurement of the laser combs were performed as the lasers were driven in continuous wave (CW) mode at cryogenic temperature employing a Fourier transform infrared spectrometer (Bruker v80). To reduce the water absorption, the beam path in the spectrometer is evacuated down to 3 mbar and the beam path outside the spectrometer is purged with dry air. The spectra shown in Figure 2c were recorded with a spectral resolution of 0.08 cm^{-1} in a fast scan mode.

Multiheterodyne dual-comb detection: The multiheterodyne dual-comb spectra shown in Figures 1c, 2a, and 5b were measured using the QCL comb itself as a fast detector. The experimental setup is shown in Figure 1a. Both Comb1 and Comb2 emit terahertz light and simultaneously Comb2 can detect the multiheterodyne beating signals [17,20,22]. Since fast detectors working around 4 THz with a bandwidth up to the GHz level are not commercially available, the self-detection technique employed here can make the fast multiheterodyne detection feasible and largely simplify the experimental setup. To extract the RF signal, a Bias-T is connected to Comb2 (detector) as shown in Figure 1a. The signal exits from the AC port of the Bias-T and then is amplified using a microwave amplifier, and finally the dual-comb spectra are registered on a spectrum analyzer (Rohde & Schwarz, FSW26). Note that in the current geometry, the two lasers are equivalent which means that either laser can be used as the fast detector for the multiheterodyne detection. As shown in Figure S5 (Supporting Information), the dual-comb spectra were obtained using Comb1 as the detector. Although either laser can be used as the detector, the measured spectra using different detectors show different line numbers and signal to noise ratios. This is because that the optical coupling in reality cannot be the same when we use different lasers as detectors. Furthermore, the QCLs can demonstrate different detection abilities due to the non-ideal growth, fabrication processes, mounting procedures, etc.

Microwave injection: The microwave injection is an efficient tool to lock the repetition rate of a semiconductor laser and then further broaden the emission spectrum, which has been widely used for mid-infrared and terahertz QCLs [24, 25, 27]. In previous studies, the microwave signal is resonantly injected to a laser at its cavity round-trip frequency. In this work, we find that the resonant injection can only work at low RF power. As the RF power is increased to some level (for example, 5 dBm using Comb2 as detector and 14 dBm using Comb1 as detector), the resonant injection will result in large phase noise and the dual-comb signal disappears then (See Video 2 in Supporting Information). Therefore, here we employ the off-resonant injection technique when the RF power is large. To extract the high-frequency signal from the laser cavity, we use a microwave transmission line. The microwave injection is only applied onto one of the lasers, for example, Comb1 as shown in Figure 1a. The microwave signal delivered from the RF generator (Rohde & Schwarz, SMA100B) is sent to Comb1 via the AC port of a Bias-T. The signal frequency and power can be precisely tuned by the RF generator. By shifting the injecting frequency from f_{BN1} , we can easily switch from resonant injection to off-resonant injection.

Supporting Information

Supporting Information is available from the author.

Acknowledgements

This work is supported by the National Natural Science Foundation of China (61875220, 62035005, 61927813, and 61991430), the “From 0 to 1” Innovation Program of the Chinese Academy of Sciences (ZDBS-LY-JSC009), the Scientific Instrument and Equipment Development Project of the Chinese Academy of Sciences (YJKYYQ20200032), the Science and Technology Commission of Shanghai Municipality (21ZR1474600), the National Science Fund for Excellent Young Scholars (62022084), Shanghai Outstanding Academic Leaders Plan (20XD1424700), and Shanghai Youth Top Talent Support Program.

Conflict of Interest

The authors declare no conflict of interest.

Data Availability Statement

The data that support the findings of this study are available from the corresponding author upon reasonable request.

References

- [1] P. Del’Haye, A. Schliesser, O. Arcizet, T. Wilken, R. Holzwarth, T. J. Kippenberg, *Nature* **2007**, *450* 1214.
- [2] T. Yasui, Y. Kabetani, E. Saneyoshi, S. Yokoyama, T. Araki, *Appl. Phys. Lett.* **2006**, *88* 241104.
- [3] T. Udem, R. Holzwarth, T. W. Hänsch, *Nature* **2002**, *416* 233.
- [4] J. Faist, G. Villares, G. Scalari, M. Rösch, C. Bonzon, A. Hugi, M. Beck, *Nanophotonics* **2016**, *5* 272.
- [5] N. Picqué, T. W. Hänsch, *Nat. Photonics* **2019**, *13* 146.

- [6] F. Cappelli, L. Consolino, G. Campo, I. Galli, D. Mazzotti, A. Campa, M. S. de Cumis, P. C. Pastor, R. Eramo, M. Rösch, M. Beck, G. Scalari, J. Faist, P. D. Natale, S. Bartalini, *Nat. Photonics* **2019**, *13* 562.
- [7] F. Keilmann, C. Gohle, R. Holzwarth, *Opt. Lett.* **2004**, *29* 1542.
- [8] Y. Yang, D. Burghoff, J. Reno, Q. Hu, *Opt. Lett.* **2017**, *42* 3888.
- [9] C. G. Wade, N. Šibalić, N. R. de Melo, J. M. Kondo, C. S. Adams, K. J. Weatherill, *Nat. Photonics* **2017**, *11* 40.
- [10] I. Coddington, N. Newbury, W. Swann, *Optica* **2016**, *3* 414.
- [11] G. Villares, A. Hugi, S. Blaser, J. Faist, *Nature Communications* **2014**, *5* 5192.
- [12] L. A. Sterczewski, J. Westberg, Y. Yang, D. Burghoff, J. Reno, Q. Hu, G. Wysocki, *ACS Photonics* **2020**, *7* 1082.
- [13] M. Rösch, G. Scalari, M. Beck, J. Faist, *Nat. Photonics* **2015**, *9* 42.
- [14] S. Barbieri, M. Ravaro, P. Gellie, G. Santarelli, C. Manquest, C. Sirtori, S. P. Khanna, E. H. Linfield, A. G. Davies, *Nat. Photonics* **2011**, *5* 306.
- [15] R. Köhler, A. Tredicucci, F. Beltram, H. E. Beere, E. H. Linfield, A. G. Davies, D. A. Ritchie, R. C. Iotti, F. Rossi, *Nature* **2002**, *417* 156.
- [16] M. Brandstetter, C. Deutsch, M. Krall, H. Detz, D. C. MacFarland, T. Zederbauer, A. M. Andrews, W. Schrenk, G. Strasser, K. Unterrainer, *Appl. Phys. Lett.* **2013**, *103* 171113.
- [17] M. Rösch, G. Scalari, G. Villares, L. Bosco, M. Beck, J. Faist, *Appl. Phys. Lett.* **2016**, *108* 171104.
- [18] G. Scalari, J. Faist, N. Picque, *Appl. Phys. Lett.* **2019**, *114* 150401.
- [19] Y. Yang, D. Burghoff, D. J. Hayton, J.-R. Gao, J. L. Reno, Q. Hu, *Optica* **2016**, *3* 499.
- [20] H. Li, Z. Li, W. Wan, K. Zhou, X. Liao, S. Yang, C. Wang, J. C. Cao, H. Zeng, *ACS Photonics* **2020**, *7* 49.
- [21] L. A. Sterczewski, J. Westberg, Y. Yang, D. Burghoff, J. Reno, Q. Hu, G. Wysocki, *Optica* **2019**, *6* 766.
- [22] Z. Li, W. Wan, K. Zhou, X. Liao, S. Yang, Z. Fu, J. Cao, H. Li, *Phys. Rev. Appl.* **2019**, *12* 044068.
- [23] K. Zhou, H. Li, W. Wan, Z. Li, X. Liao, J. Cao, *Appl. Phys. Lett.* **2019**, *114* 191106.
- [24] H. Li, P. Laffaille, D. Gacemi, M. Apfel, C. Sirtori, J. Leonardon, G. Santarelli, M. Rösch, G. Scalari, M. Beck, J. Faist, W. Hänsel, R. Holzwarth, S. Barbieri, *Opt. Express* **2015**, *23* 33270.
- [25] C. Y. Wang, L. Kuznetsova, V. M. Gkortsas, L. Diehl, F. X. Kartner, M. A. Belkin, A. Belyanin, X. Li, D. Ham, H. Schneider, P. Grant, C. Y. Song, S. Haffouz, Z. R. Wasilewski, H. C. Liu, F. Capasso, *Opt. Express* **2009**, *17* 12929.

- [26] E. Rodriguez, A. Mottaghizadeh, D. Gacemi, M. Jeannin, Z. Asghari, A. Vasanelli, Y. Todorov, Q. J. Wang, C. Sirtori, *Laser Photonics Rev.* **2020**, *14* 1900389.
- [27] P. Gellie, S. Barbieri, J.-F. Lampin, P. Filloux, C. Manquest, C. Sirtori, I. Sagnes, S. P. Khanna, E. H. Linfield, A. G. Davies, H. Beere, D. Ritchie, *Opt. Express* **2010**, *18* 20799.
- [28] W. Wan, H. Li, T. Zhou, J. Cao, *Sci. Rep.* **2017**, *7* 44109.
- [29] R. Rungsawang, N. Jukam, J. Maysonnave, P. Cavalie, J. Madeo, D. Oustinov, S. S. Dhillon, J. Tignon, P. Gellie, C. Sirtori, S. Barbieri, H. E. Beere, D. A. Ritchie, *Appl. Phys. Lett.* **2011**, *98* 101102.
- [30] H. Li, J. M. Manceau, A. Andronico, V. Jagtap, C. Sirtori, L. H. Li, E. H. Linfield, A. G. Davies, S. Barbieri, *Appl. Phys. Lett.* **2014**, *104* 241102.
- [31] S. Barbieri, M. Ravaro, P. Gellie, G. Santarelli, C. Manquest, C. Sirtori, S. P. Khanna, E. H. Linfield, A. G. Davies, *Nat. Photonics* **2011**, *5* 306.
- [32] D. Oustinov, N. Jukam, R. Rungsawang, J. Madéo, S. Barbieri, P. Filloux, C. Sirtori, X. Marcadet, J. Tignon, S. Dhillon, *Nat. Commun.* **2010**, *1* 69.
- [33] H. Li, M. Yan, W. Wan, T. Zhou, K. Zhou, Z. Li, J. Cao, Q. Yu, K. Zhang, M. Li, J. Nan, B. He, H. Zeng, *Adv. Sci.* **2019**, *6* 1900460.
- [34] Y. Zhao, Z. Li, K. Zhou, X. Liao, W. Guan, W. Wan, S. Yang, J. Cao, D. Xu, S. Barbieri, H. Li, *Laser Photonics Rev.* **2021**, *15* 2000498.